NASA TECHNICAL MEMORANDUM

NASA TM X-1807

NASA TM X-1807

QUIESCENT-AIR PERFORMANCE OF A TRUNCATED TURBOJET PLUG NOZZLE WITH SHROUD AND PLUG BASE FLOWS FROM A COMMON SOURCE

by Albert L. Johns

Lewis Research Center
Cleveland, Ohio

NATIONAL AERONAUTICS AND SPACE ADMINISTRATION • WASHINGTON, D. C. • JUNE 1969

NASA TM X-1807

QUIESCENT-AIR PERFORMANCE OF A TRUNCATED TURBOJET PLUG NOZZLE WITH SHROUD AND PLUG BASE FLOWS FROM A COMMON SOURCE

By Albert L. Johns

Lewis Research Center
Cleveland, Ohio

NATIONAL AERONAUTICS AND SPACE ADMINISTRATION

For sale by the Clearinghouse for Federal Scientific and Technical Information
Springfield, Virginia 22151 – CFSTI price $3.00

ABSTRACT

A 10^{o} half-angle conical plug nozzle with a design pressure ratio of 26.3 and a 50-percent plug truncation was tested in configurations simulating afterburner on and off. A 40-percent increase in primary throat area was provided by either a simulated primary iris flap or by relative translation between the primary shroud and plug. Thrust efficiency was maintained at values between 97 and 99 percent over a range of pressure ratios by proper location of the cylindrical outer shroud. These peak efficiencies were generally obtained with the sum of shroud and plug base flows from 5 to 7 percent of the primary flow.

CONTENTS

QUIESCENT-AIR PERFORMANCE OF A TRUNCATED TURBOJET PLUG NOZZLE WITH SHROUD AND PLUG BASE FLOWS FROM A COMMON SOURCE

by Albert L. Johns

Lewis Research Center

SUMMARY

An experimental investigation was conducted in the Lewis Research Center's nozzle static test facility to determine the nonafterburning and afterburning performance characteristics of a 50-percent truncated, 10^{o} half-angle conical plug nozzle. The turbojet plug nozzle was designed for an overall pressure ratio of 26.3. Shroud and plug base flows with total weight-flow rates as high as 22.3 percent of the primary flow were supplied from a common source. Two methods of varying the primary throat area for afterburning were evaluated: a simulated primary iris flap, and relative translation between the primary shroud and the plug surface. The internal expansion of the nozzle was varied by translating a cylindrical outer shroud.

By proper location of the external shroud, static thrust efficiency was maintained at values between 97 and 99 percent over a range of pressure ratios. These peak efficiencies were generally obtained with the sum of shroud and plug base flows from 5 to 7 percent of the primary flow. For the secondary-flow system investigated, about 80 percent of the total flow was exhausted between the primary and secondary shrouds, while the remaining 20 percent was exhausted into the plug base. None of the configurations tested would pump cooling flow at takeoff with the external shroud fully retracted to obtain peak thrust efficiency.

INTRODUCTION

In the continuing program in airbreathing propulsion at the Lewis Research Center, plug nozzles are receiving considerable emphasis because they may offer the potential of good aerodynamic performance together with less complexity and a consequent reduction in maintenance problems. References 1 to 3 document the aerodynamic performance of low-angle plug nozzle configurations with translating cylindrical outer shrouds suitable

for both nonafterburning and afterburning turbojet engines designed for aircraft cruising at a Mach number near 2.7. A high level of nozzle efficiency was maintained over a wide range of pressure ratio and Mach number by extending the outer shroud to control the internal expansion as nozzle pressure ratio increased.

To provide for changes in engine operating conditions, such as afterburning, the nozzle must have a variable primary throat area. This area variation can be accomplished in several ways with a plug nozzle. It can have an iris primary (ref. 2), relative translation between the primary shroud and the plug (ref. 3), or a variable-diameter plug (ref. 4). For afterburning engines, cooling flow may be required for the primary and secondary shrouds as well as for the plug surface and its support structure. The thrust and pumping characteristics of a plug nozzle with secondary flow for primary and secondary shroud cooling are presented in references 2 and 3. Plug truncation is desirable to minimize the heat load on the plug surface cooling system and to minimize length. It has been demonstrated in references 1, 2, and 5 that at least 25 percent of the plug length can be removed without producing significant performance losses. If greater truncations are used, bleed flow in the base of the plug tends to minimize the loss in performance (ref. 1). The results presented in reference 1 also indicate a small effect of external flow on the pumping characteristics of plug base bleed, so that static data can be of value.

This report presents the static thrust and pumping characteristics of the truncated low-angle plug nozzles reported in references 2 and 3 with secondary and plug base flows supplied from a common auxiliary source. These nozzles feature a rigid 10° half-angle conical plug with 50-percent truncation, a simulated translating outer cylindrical shroud, and an overall design pressure ratio of 26.3. A 40-percent increase in primary throat area was provided for afterburning by either a simulated iris flap or translation between the primary shroud and plug surface. Dry air at room temperature was used for primary and auxiliary flows. The sum of shroud and plug base flows was studied at rates as high as 22.3 percent of the primary flow over a range of nozzle pressure ratio from about 2 to 29. The nozzle was investigated in the Lewis Research Center's nozzle static test stand.

SYMBOLS

A area

d model diameter

F thrust

M Mach number

P total pressure

p	static pressure
T	total temperature
w	weight-flow rate
$\frac{w_b}{w_p}\sqrt{\frac{T_b}{T_p}}$	corrected base-weight-flow-rate ratio
$\frac{w_s}{w_p}\sqrt{\frac{T_s}{T_p}}$	corrected secondary-weight-flow-rate ratio
x	axial distance measured from nozzle throat to external shroud lip
θ	circumferential position, deg

Subscripts:

a	auxiliary
av	average
b	base
bt	primary nozzle boattail
i	ideal
j	jet
max	maximum
min	minimum
p	primary
s	secondary
0	ambient
7	nozzle inlet
8	nozzle throat
9	nozzle exit

Superscript:

$\bar{}$	average value

APPARATUS AND PROCEDURE

Installation in Static Test Facility

The research hardware installation in the static test facility is shown in figures 1 and 2. The nozzles were installed in a test chamber that was connected to the laboratory combustion air and altitude exhaust facilities. The nozzles were mounted from an adapter section that contained a bellmouth inlet for the primary air supply. The adapter section was rigidly attached to a bedplate that was freely suspended by four flexure rods. Both external and internal pressure forces acting on the nozzle, bellmouth, and adapter were transmitted from the bedplate through a bell crank to a calibrated balanced-air-pressure diaphragm which was used in measuring thrust. A labyrinth seal around the inlet section ahead of the adapter sealed the primary inlet air from the exhaust plenum chamber. The space between the two labyrinth seals was vented to the test chamber. This decreased the pressure differential across the second labyrinth seal and prevented a pressure gradient on the outside of the diffuser section caused by an air blast from under the labyrinth seal.

The nozzle primary airflow was calculated from pressure and temperature measurements at the air-metering station (fig. 1) and an effective area determined by an ASME calibration nozzle. The total auxiliary airflow w_a was measured by means of a standard ASME flowmetering orifice in the external supply line. This flow split inside the model (fig. 3) to supply secondary flow w_s for the primary and secondary shrouds and base bleed flow w_b for the plug. The effects on performance of variations in auxiliary flow were obtained in this study without regard to the cooling requirements of the nozzle. In an actual application, however, the auxiliary flow rates for performance and for cooling purposes would be optimized.

It was determined that about 80 percent of the total auxiliary flow entered the secondary passage in this particular model, while the remaining 20 percent went into the base, as shown in figure 4. This split was approximately proportional to the ratio of minimum flow areas within the secondary and plug base-flow passages. The secondary flow w_s was estimated by using the pumping characteristics of a similar nozzle presented in references 2 and 3. The base flow w_b was then calculated as the difference between the total and secondary flows.

Nozzle Instrumentation

Primary, secondary, and base total pressures were measured with pitot probes, as shown in figure 3. The primary total pressure was measured with two area-weighted

rakes located at meridian angles of 120° and 300°. The total-pressure distortion parameter $(P_{7,\max} - P_{7,\min})/P_{7,av}$ varied from 0.025 with the afterburner off to 0.050 with the afterburner on. A thermocouple and two static-pressure orifices were located at each of the primary rakes. The secondary system consisted of one pitot probe and a thermocouple at meridian angles of 0° and 90° and a static-pressure orifice at 10° and 100°. The total-pressure distortion parameter had a maximum value of 0.045 at the highest auxiliary flow rate. The base-flow system contained one pitot probe at the centerline and a thermocouple at a meridian angle of 0° (fig. 3). The plug base exit contained a static-pressure orifice at 90° and one at 270°. Each primary shroud boattail contained two rows of three area-weighted static-pressure orifices located at meridian angles of 180° and 270°.

Nozzle Configurations

The nozzle configurations had a 10° half-angle conical plug truncated to one-half of its total length from the throat station (fig. 5). The afterburner-off configuration (fig. 5(a)) had a throat area that was 26 percent of the overall nozzle projected area, based on a model diameter of 21.59 centimeters. The overall design pressure ratio of this configuration was 26.3, based on the ratio of nozzle exit area to throat area A_9/A_8 (internal area ratio) of 2.91.

The afterburner-off primary nozzle shroud had a 17.5° boattail angle and a projected area equal to 24 percent of the maximum model area. A 40-percent increase in primary throat area was provided for afterburning by either a simulated iris flap (fig. 5(b)) or by relative translation between the primary shroud and plug surface (fig. 5(c)). Both afterburning configurations had a ratio of throat to maximum model area of 0.368. The primary nozzle shroud for the iris configuration (fig. 5(b)) had a 7.6° boattail angle and a projected area equal to 15 percent of the maximum model area. The primary nozzle shroud for the translated configuration (fig. 5(c)) was identical to that with the afterburner off.

Three cylindrical outer shrouds of varying lengths were used to simulate translation. The shroud extensions tested are shown in figure 5 for both the afterburner-off and afterburner-on configurations. The resulting internal area ratios and the corresponding pressure ratios are listed in table I. Nozzle exit area A_9 was defined as the annular flow area between the outer cylindrical shroud exit and the plug surface for the fully extended and partially extended configurations. When the external shroud is fully retracted, the nozzle exit area A_9 is defined as the annular flow area between the primary shroud exit and the plug, and hence is identical to A_8.

Force Measurements

Actual jet thrust was calculated from load cell measurements corrected for tare forces. The ideal jet thrust for each of the three flows was calculated from the measured mass-flow rate expanded from their measured total pressures (P_7, P_s, P_b) to p_0. Provision was made to equate the ideal thrust of the secondary or base flow to zero if their total pressure was less than p_0. Review of the data following the test program indicated that this did not occur for the results presented in this report. Nozzle efficiency is therefore defined as the ratio of the actual jet thrust to the combined ideal thrust of the primary, secondary, and base flows:

$$\text{Nozzle efficiency} = \frac{F_j}{F_{i,p} + F_{i,s} + F_{i,b}}$$

In addition to the efficiency parameter, the data are also presented in the form of nozzle gross thrust coefficient $F_j/F_{i,p}$.

The thrust system was calibrated by using standard ASME sonic nozzles with various throat sizes. The performance is shown in figure 6 for two of these ASME nozzles with throat areas nearly equal to the afterburner-off and afterburner-on throat areas studied herein. The measured performance was compared with theoretical performance calculated from ASME discharge and velocity coefficients of 0.9935 and 0.996, respectively, taken from reference 6. The results indicate approximately a ±2-percent scatter in force measurements with the smaller throat area (fig. 6(a)) and approximately a ±1-percent scatter with the larger throat (fig. 6(b)).

The percent error in jet thrust measurements in this facility is directly related to the ratio of nozzle throat to adapter diameter. For nozzles with relatively small throat areas, the jet thrust is small compared to either the load cell reading or the external tare force. Small errors in either of these large measured forces are magnified in the smaller calculated jet thrust. As nozzle throat size increases, the external tare force decreases, and the jet thrust increases and becomes a larger fraction of the load cell reading. Small errors in measured forces are therefore not magnified significantly for nozzles with relatively large throat areas.

Procedure

Nozzle pressure ratios were set by maintaining a constant nozzle inlet pressure P_7 and varying the tank pressure p_0 with the use of exhausters. The partially and fully extended shroud configurations were tested over a range of pressure ratios above and

below the internal pressure ratio value listed in table I. The fully retracted shroud configurations were tested above the internal pressure ratio value listed in table I. The total-pressure-recovery requirements presented herein for the secondary- and base-flow systems were calculated by using the schedule of assumed pressure ratio against Mach number shown in figure 7 for an afterburning turbojet engine.

RESULTS AND DISCUSSION

Performance and Pumping Characteristics

A nonafterburning and two afterburning configurations were tested with three outer cylindrical shrouds of varying length to simulate translation. All configurations were tested over a range of primary total-pressure ratios and auxiliary flows. The measured static-thrust efficiency and pumping characteristics are presented in figure 8. Although the scatter of force data for the small primary nozzle obscured detailed effects of the variables, general trends were fairly clear and consistent with those of the large nozzles.

Afterburner off. - With the two shroud extensions, peak nozzle efficiency with the afterburner off (fig. 8(a)) was generally obtained at a pressure ratio higher than the internal expansion value and at corrected total auxiliary flow rates from 6 to 12 percent of the primary flow. The fully extended shroud provided a high level of efficiency (97 percent) for supersonic aircraft cruising near Mach 2.7 at a pressure ratio of about 29. The fully retracted shroud configuration was about 98 percent efficient at a dry takeoff pressure ratio near 3.0. The partially extended shroud was a poor configuration for the intermediate pressure ratio range when compared with the fully extended shroud at the same pressure ratios. It is probable that the partially extended shroud was not extended far enough to control the expansion of the primary and secondary flows. This lack of control resulted in excessive overexpansion and divergence losses at the shroud discharge. When the fully extended and partially extended shroud configurations are operating below the internal pressure ratio, the nozzle efficiency can be improved considerably by increasing corrected auxiliary weight flow from 0 to 6 percent of the primary weight flow. The results presented in figure 8(a) indicate that a two-position shroud (fully extended or fully retracted) may be of some interest for this pressure ratio range. However, external flow affects nozzle performance and must also be considered when selecting optimum shroud extension. References 2 and 3 present the preformance of the low-angle plug nozzles studied herein over a range of Mach numbers from 0 to 2.0.

Pumping characteristics for both the secondary- and base-flow systems are presented in figure 8(a) for combined flow rates as high as 22.3 percent of the primary flow. As mentioned previously, 80 percent of the total flow went into the secondary while the

remaining 20 percent went into the plug base. Both secondary and base total-pressure ratios were generally insensitive to nozzle pressure ratio for the partially and fully extended shrouds and constant weight-flow ratios. This was not true at low pressure ratio with the shroud fully retracted. The insensitivity of secondary and base pressure ratios to shroud location indicates choking in both the secondary and base systems, particularly at pressure ratios associated with the partially extended and fully extended shrouds. The foregoing insensitivity effects were also observed with the fully retracted shroud at the higher pressure ratios. In general, a higher total pressure was required to pump the same weight-flow rate through the base than through the secondary system.

Afterburner on (iris flap). - To simulate afterburner-on operation with an iris flap, the boattail angle of the afterburner-off configuration was decreased to 7.6°, producing a 40-percent increase in throat area and a 54.2-percent decrease in primary shroud boattail area. The nozzle efficiency and pumping characteristics are shown in figure 8(b) for three shroud locations and a range of corrected total auxiliary weight-flow ratios. The peak efficiency generally occurred with about 6-percent corrected total auxiliary weight flow and with overall nozzle pressure ratios near the value of the internal pressure ratio. Performance generally was higher than with the afterburner off, because of a lower primary shroud boattail angle and projected area. The peak efficiency at supersonic cruise with the shroud fully extended was about 98 percent. The performance at takeoff was also about 98.5 percent with the shroud fully retracted. The performance with the partially extended shroud was improved over that obtained with the afterburner off, from 93.5 to about 98 percent. Although an increase in the partially extended shroud performance occurred, a two-position shroud still seems attractive. The nozzle efficiency can be improved considerably at nozzle pressure ratios below the internal pressure ratio with both shroud extensions, by increasing the corrected total auxiliary weight flow from 0 to 6 percent of the primary weight flow. The pumping characteristics for this iris-type afterburning configuration indicate that higher secondary and base total-pressure ratios are required to pump equivalent mass-flow rates when compared with the afterburner-off configuration (fig. 8(a)). This requirement is due to the geometric choking and the higher primary-flow rates of the afterburning configuration.

Afterburner on (translating primary). - For the alternate afterburner-on configuration, the primary nozzle flap of the afterburner-off configuration was translated downstream to provide a 40-percent increase in throat area. The shroud extension ratios for this configuration are less than the preceding two configurations since the same external shrouds were used. In fact, the partially extended shroud was nearly alined with the end of the primary flap, as shown in figure 5(c). Optimum nozzle efficiency (fig. 8(c)) with the fully extended shroud was obtained with about 7-percent corrected total auxiliary weight-flow ratio. Secondary flow was less effective with the partially extended shroud and the fully retracted shroud. Peak nozzle efficiencies were high for these configura-

tions, but were still about 2 percent lower than the iris afterburning data with the shroud extended. Reference 3 indicates that external flow reduces the nozzle efficiency with the partially extended shroud. Apparently, the partially extended shroud is not extended far enough to control the primary-flow expansion. There is also a large primary nozzle boattail drag. The fully extended shroud nozzle efficiency can be improved at nozzle pressure ratios below the internal pressure ratio, by increasing the corrected total auxiliary weight flow from 0 to 7 percent of the primary weight flow. The pumping characteristics of this afterburning configuration with a translating primary shroud are similar to those obtained with the iris-type primary (fig. 8(b)).

The gross thrust coefficients for all nozzle configurations are presented in figure 9 over a range of nozzle total-pressure ratio for corrected auxiliary flow rates as high as 22.3 percent of the primary flow. As expected, gross thrust coefficient increases with increasing values of auxiliary flow.

The pumping characteristic curves from figure 8 were used in conjunction with the assumed pressure ratio schedule in figure 7 to estimate the total-pressure-recovery requirements for the secondary and base flows. These requirements are presented in figure 10. The total-pressure-recovery requirements are shown for the nonafterburning and the two afterburning configurations at several free-stream Mach numbers and appropriate values of nozzle pressure ratio and external shroud location. The secondary and base flows are choked for the fully and partially extended shrouds at low flow rates, as indicated by a linear weight-flow to pressure-recovery relation. When the shroud is fully retracted, these flows appear to be choked at the higher flow rates. As expected, the results in figure 10 indicate that the fully retracted shroud configurations do not pump cooling flow at takeoff.

Effect of Secondary and Base Flow

The effect of secondary flow on the primary nozzle boattail pressures is shown in figure 11 for the nonafterburning and two afterburning configurations for each of the three shroud positions. The relation of average boattail pressure to free-stream static pressure and to secondary total pressure is shown at a nozzle total-pressure ratio near the internal expansion value. With the shroud fully extended (fig. 11(a)), the boattail pressures are generally higher than ambient pressure. The peak boattail pressure ratio occurs at low weight-flow ratio and low velocity. For the afterburning configurations, higher boattail pressures were measured for the iris-type primary. Supersonic velocities are generally obtained with high secondary-weight-flow ratios, and boattail pressures are lower than the peak value.

With the shroud in the partially extended position (fig. 11(b)), the boattail was not pressurized as greatly as with the shroud fully extended. Peak base pressures again

were obtained at low weight-flow rates and low velocities. The iris-type primary with the afterburner on again had higher boattail pressures than the translating primary. For the latter configuration, the shroud was nearly alined with the end of the primary flap (fig. 5(c)), and boattail pressures for this configuration are lower than ambient for the range of secondary flows studied. Again, supersonic Mach numbers were obtained with these three configurations at the higher values of corrected secondary-weight-flow ratio.

With the shroud fully retracted (fig. 11(c)), boattail pressures were nearly ambient regardless of secondary-flow ratio. Supersonic speeds were indicated at the highest values of corrected secondary-weight-flow ratio studied.

The effect of base flow on the static pressure at the discharge of the plug base is shown in figure 12 for all configurations tested. It should be noted that secondary flow was also changing and was in a position to affect the plug base conditions. The relation of average plug exit static pressure to both free-stream static pressure and to base-flow total pressure is shown for a nozzle total-pressure ratio near the internal expansion value. Both the nonafterburning and iris-type afterburning configurations had exit static pressures greater than ambient with the shroud fully extended (fig. 12(a)). The iris-type afterburning configuration had higher exit pressures than the translating primary. Supersonic exit velocities are indicated at the higher values of corrected base-weight-flow ratio.

For the partially extended shroud (fig. 12(b)), the exit static pressures, in general, were less than ambient and insensitive to base-flow ratio. Again, the iris-type afterburning configuration had higher exit pressures than the translating type. Supersonic exit flow velocities again were obtained at the higher values of corrected base-weight-flow ratios.

With the shroud fully retracted (fig. 12(c)), the plug exit flow was always subsonic. Exit static pressures were nearly ambient and increased slightly with base flow.

SUMMARY OF RESULTS

An experimental investigation was conducted to determine the static performance of a truncated plug nozzle designed for an overall pressure ratio of 26.3. Shroud and plug base flows were supplied from a common source and were as much as 22.3 percent of the primary flow. Two methods of varying the primary throat area for afterburning were evaluated. Internal expansion was adjusted by translating a cylindrical outer shroud. The following results were obtained:

1. Static thrust efficiency was maintained at values between 97 and 99 percent, over a range of pressure ratios, by proper location of the cylindrical external shroud. These peak thrust efficiencies were generally obtained with a total auxiliary flow rate of about

5 to 7 percent of the primary flow For the auxiliary flow system investigated, about 80 percent of the flow was available for the secondary flow between the primary and secondary shrouds; the remaining 20 percent was available for plug base flow.

2. None of the configurations tested would pump cooling flow at takeoff with the external shroud retracted for peak thrust efficiency.

Lewis Research Center,
National Aeronautics and Space Administration,
Cleveland, Ohio, December 11, 1968,
126-15-02-10-22.

REFERENCES

1. Bresnahan, Donald L.; and Johns, Albert L.: Cold Flow Investigation of a Low Angle Turbojet Plug Nozzle With Fixed Throat and Translating Shroud at Mach Numbers From 0 to 2.0. NASA TM X-1619, 1968.

2. Bresnahan, Donald L.: Experimental Investigation of a 10^{o} Conical Turbojet Plug Nozzle With Iris Primary and Translating Shroud at Mach Numbers From 0 to 2.0. NASA TM X-1709, 1968.

3. Bresnahan, Donald L.: Experimental Investigation of a 10^{o} Conical Turbojet Plug Nozzle With Translating Primary and Secondary Shrouds at Mach Numbers From 0 to 2.0. NASA TM X-1777, 1969.

4. Wasko, Robert A.; and Harrington, Douglas E.: Performance of a Collapsible Plug Nozzle Having Either Two-Position Cylindrical or Variable Angle Floating Shrouds at Mach Numbers From 0 to 2.0. NASA TM X-1657, 1968.

5. Schmeer, James W.; Kirkham, Frank S.; and Salters, Leland B., Jr.: Performance Characteristics of a 10^{o} Conical Plug Nozzle at Mach Numbers Up to 1.29. NASA TM X-913, 1964.

6. Anon.: Fluid Meters, Their Theory and Application. Fifth ed., ASME, 1959.

TABLE I. - SECONDARY SHROUD VARIABLES

Primary nozzle configuration	Shroud extension ratio, x/d_{max}	Internal expansion pressure ratio, P_7/p_9	Internal area ratio, A_9/A_8
Afterburner off	0.618	21.10	2.99
	.215	16.06	2.54
	-.235	1.90	1.00
Afterburner on (iris)	0.618	11.93	2.13
	.215	8.87	1.81
	-.235	1.90	1.00
Afterburner on (translating)	0.338	11.93	2.13
	.058	9.89	1.91
	-.243	1.90	1.00

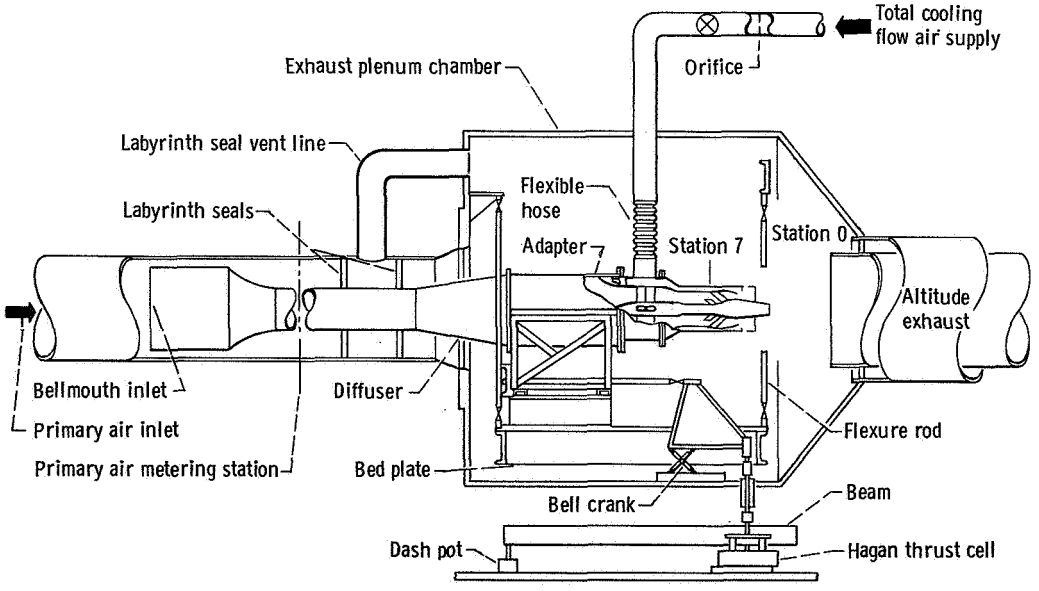

CD-10263-28

Figure 1. - Schematic view of nozzle installation in static test facility.

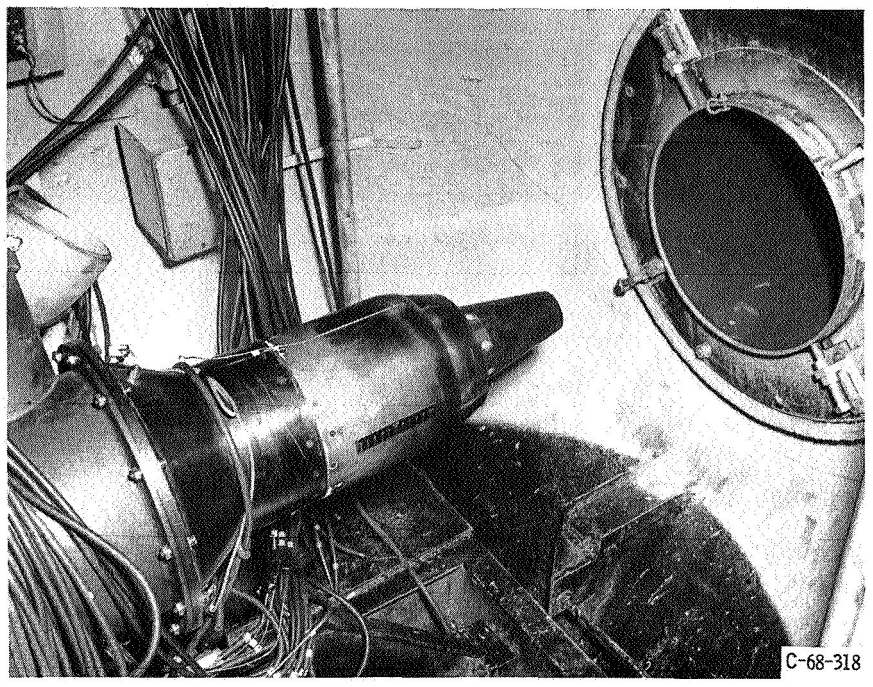

Figure 2. - Truncated plug nozzle installed in static test stand.

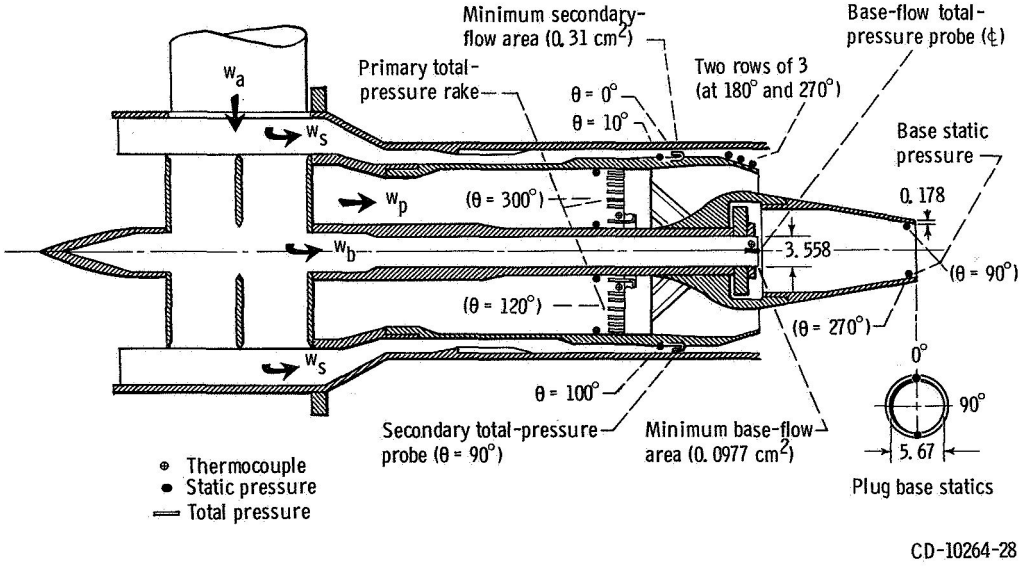

Figure 3. - Model instrumentation and weight-flow channels. (All dimensions are in centimeters unless otherwise noted.)

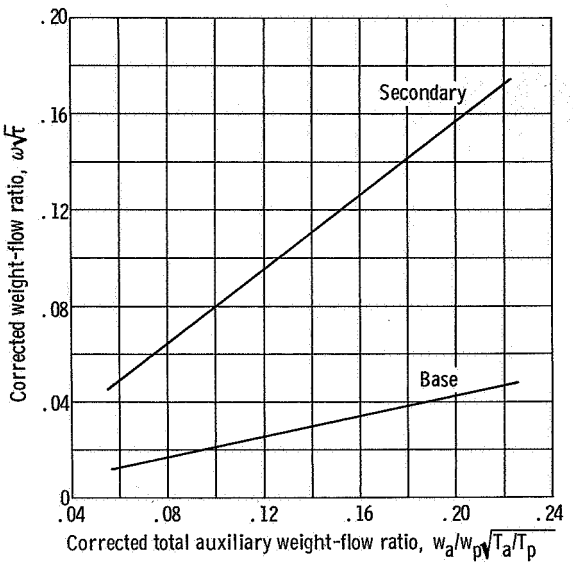

Figure 4. - Split of total cooling flow into secondary and base flows.

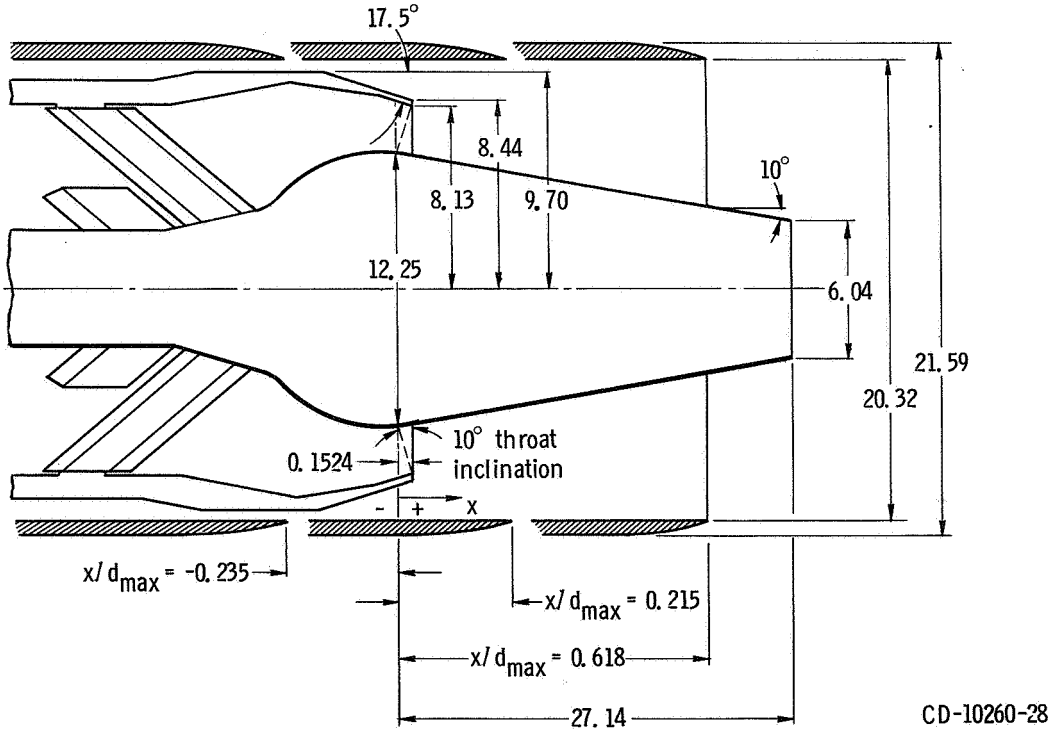

(a) Afterburner off; nozzle throat area, 94.5 square centimeters.

Figure 5. - Model dimensions and geometric variables. (All dimensions are in centimeters unless otherwise noted.)

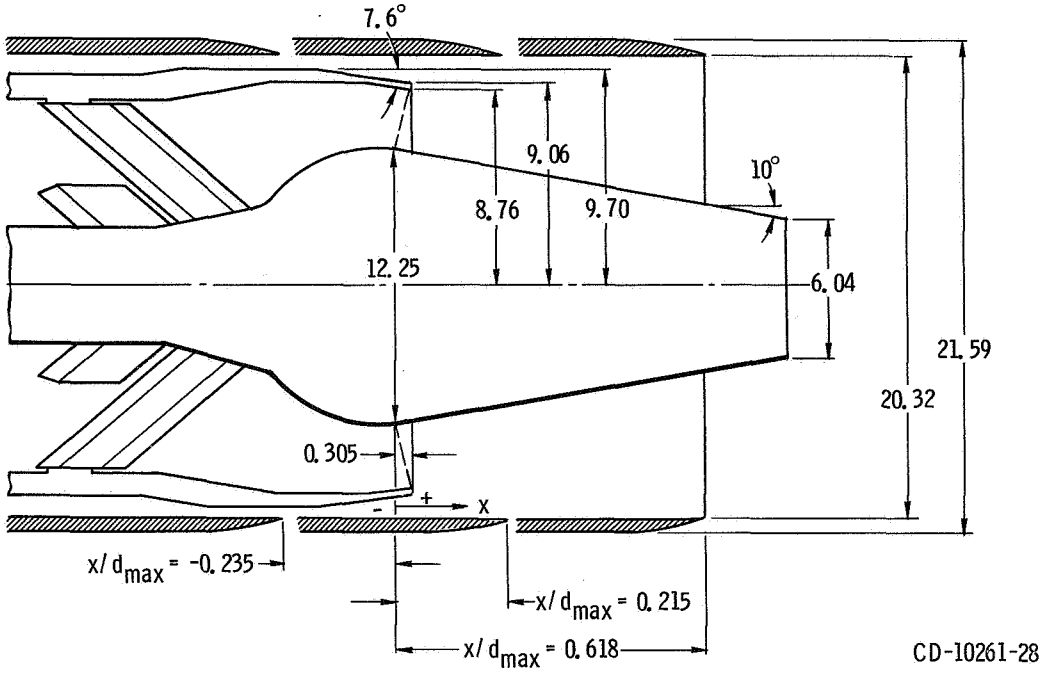

(b) Afterburner on (iris); nozzle throat area, 132.2 square centimeters.

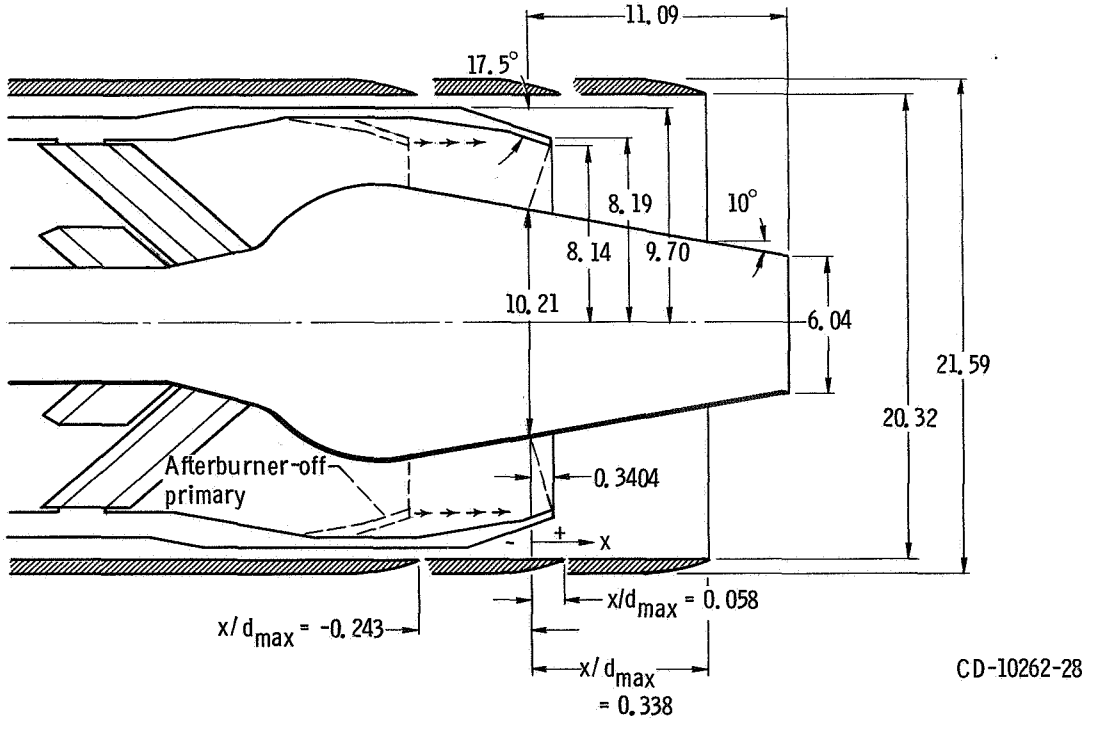

(c) Afterburner on (translating); nozzle throat area, 132.2 square centimeters.

Figure 5. - Concluded.

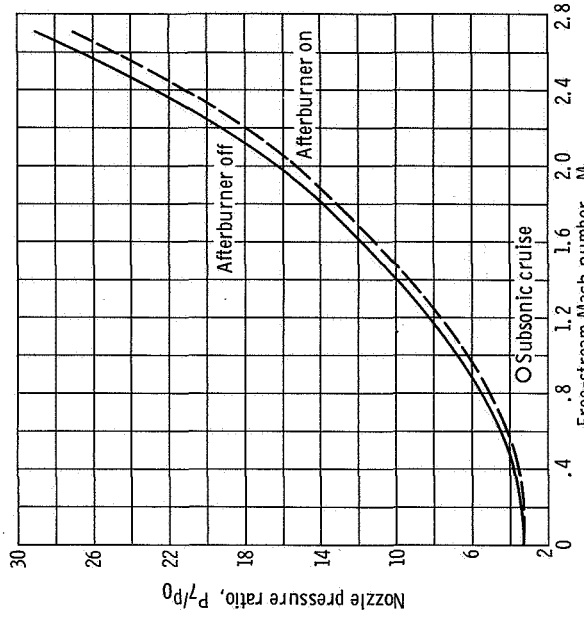

Figure 7. - Assumed pressure ratio schedule for afterburning turbojet engine.

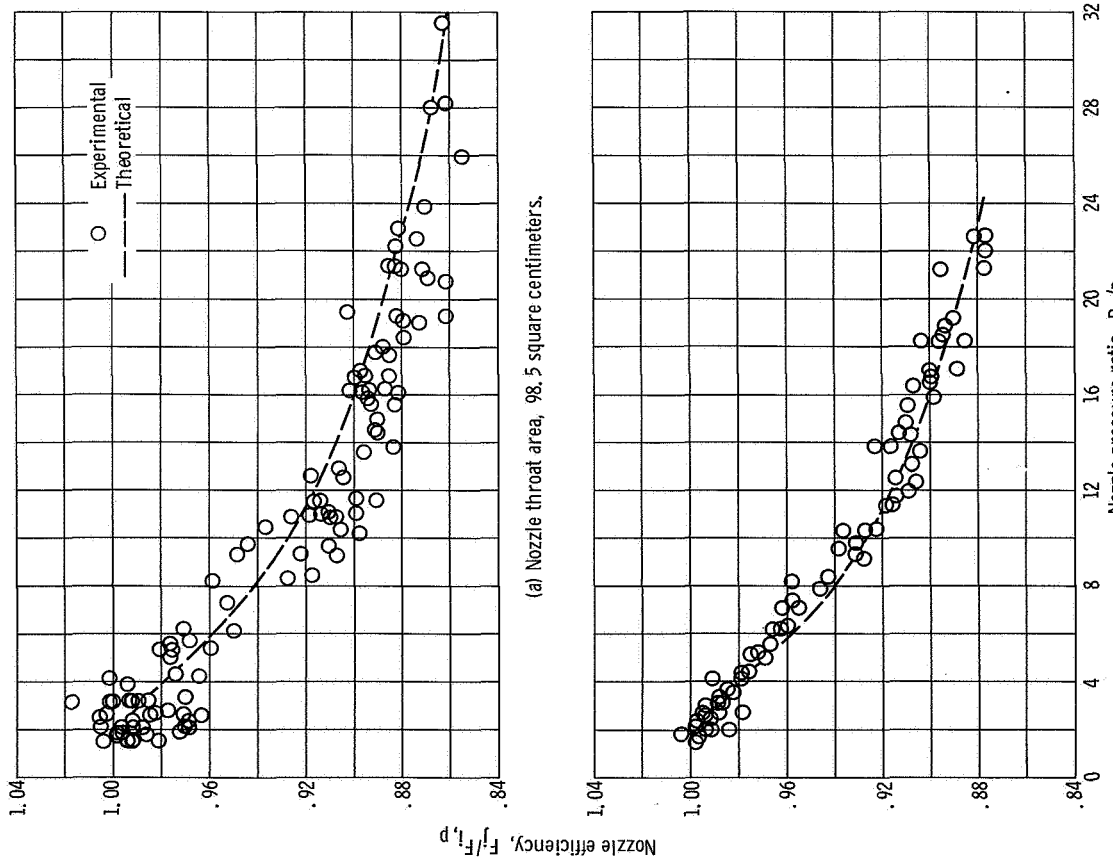

(a) Nozzle throat area, 98.5 square centimeters.

(b) Nozzle throat area, 153.2 square centimeters.

Figure 6. - Static performance of ASME sonic nozzle in static test stand.

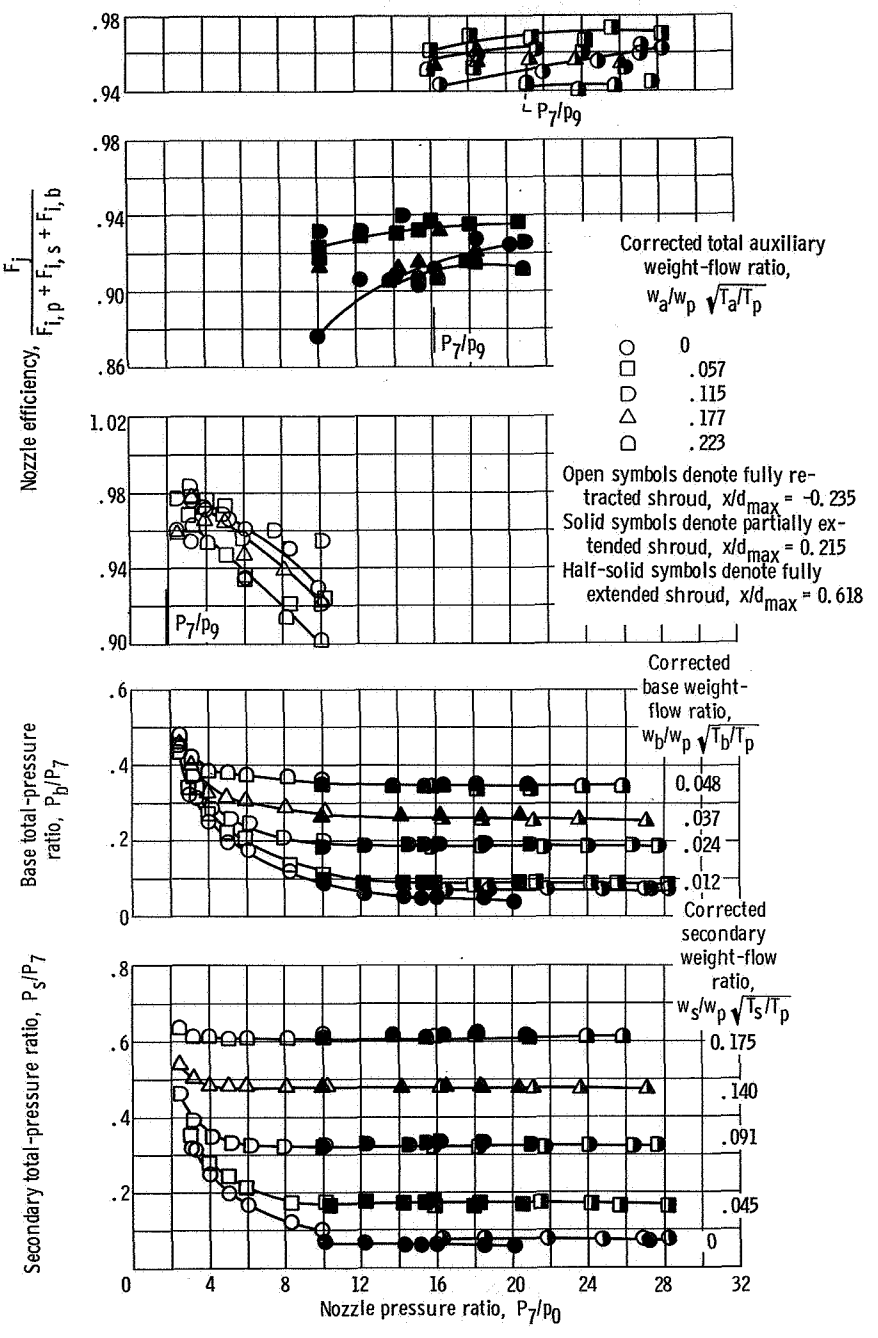

(a) Afterburner off.

Figure 8. - Nozzle efficiency and pumping characteristic curves.

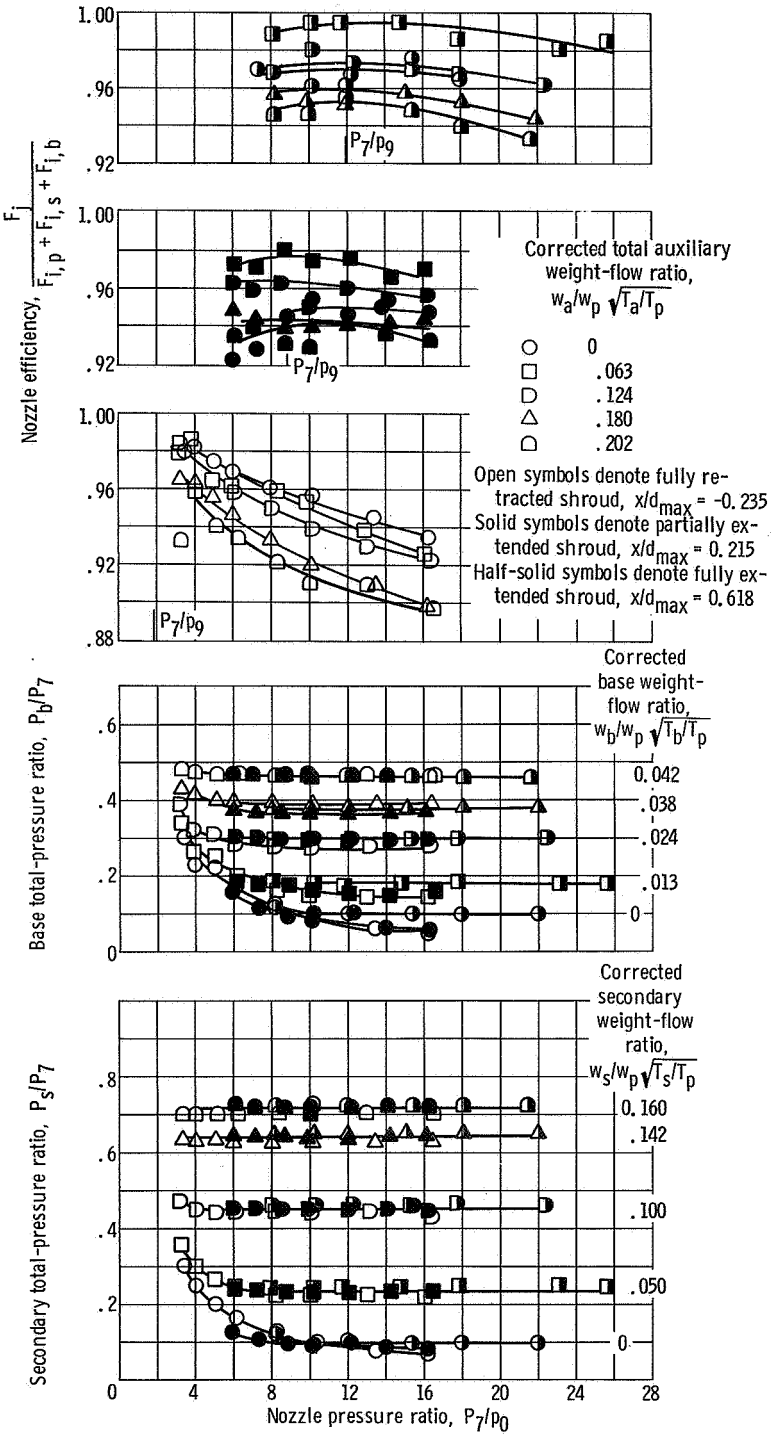

(b) Afterburner on (iris).

Figure 8. - Continued.

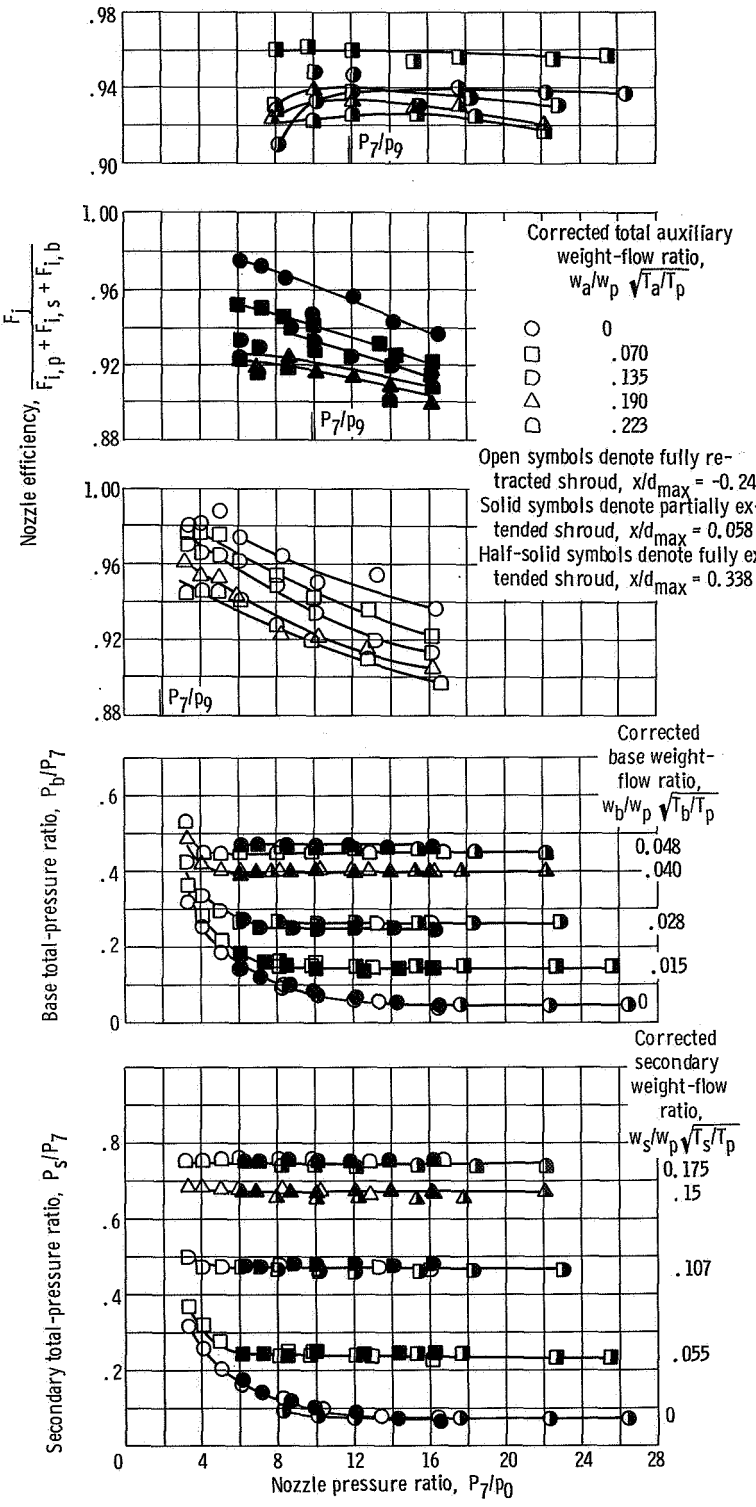

(c) Afterburner on (translating).

Figure 8. - Concluded.

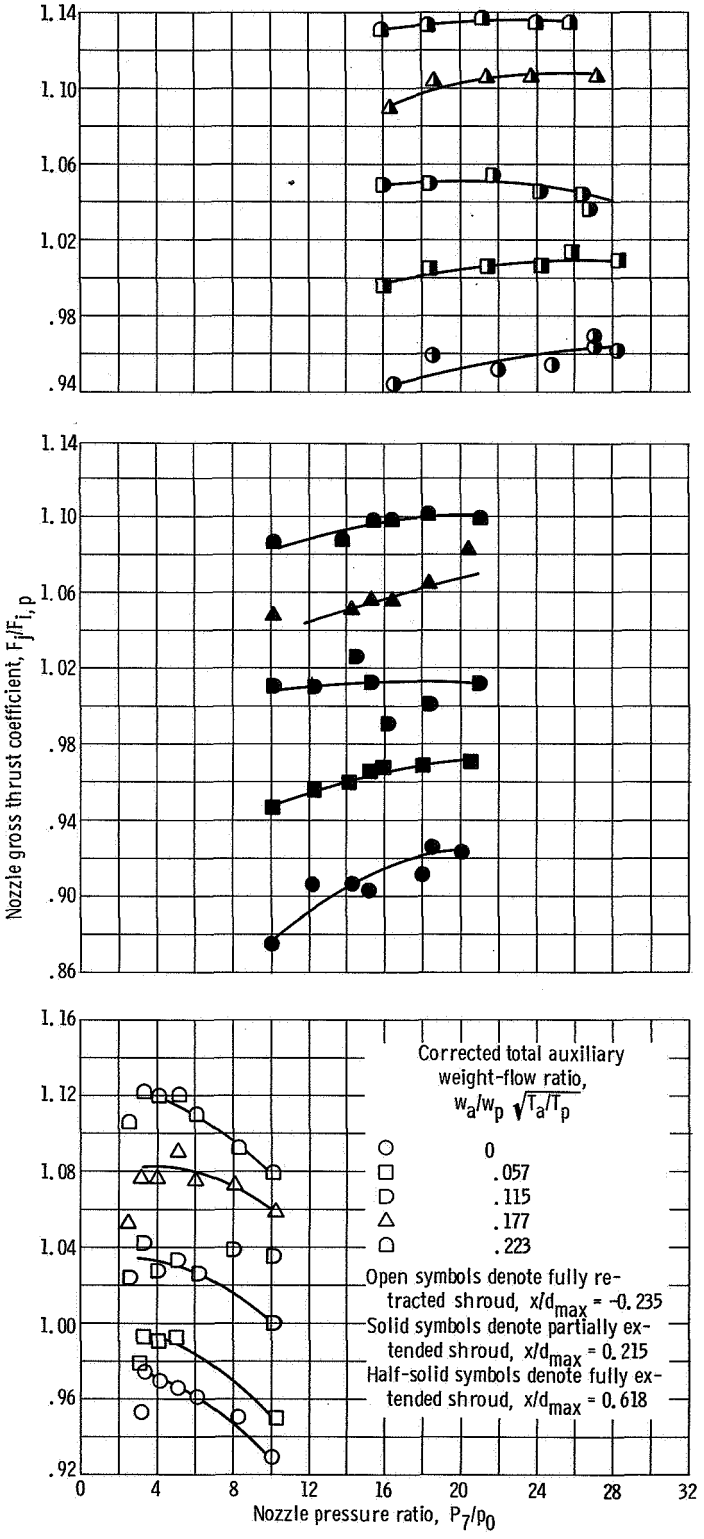

(a) Afterburner off.

Figure 9. - Effect of nozzle pressure ratio on nozzle cross thrust coefficient.

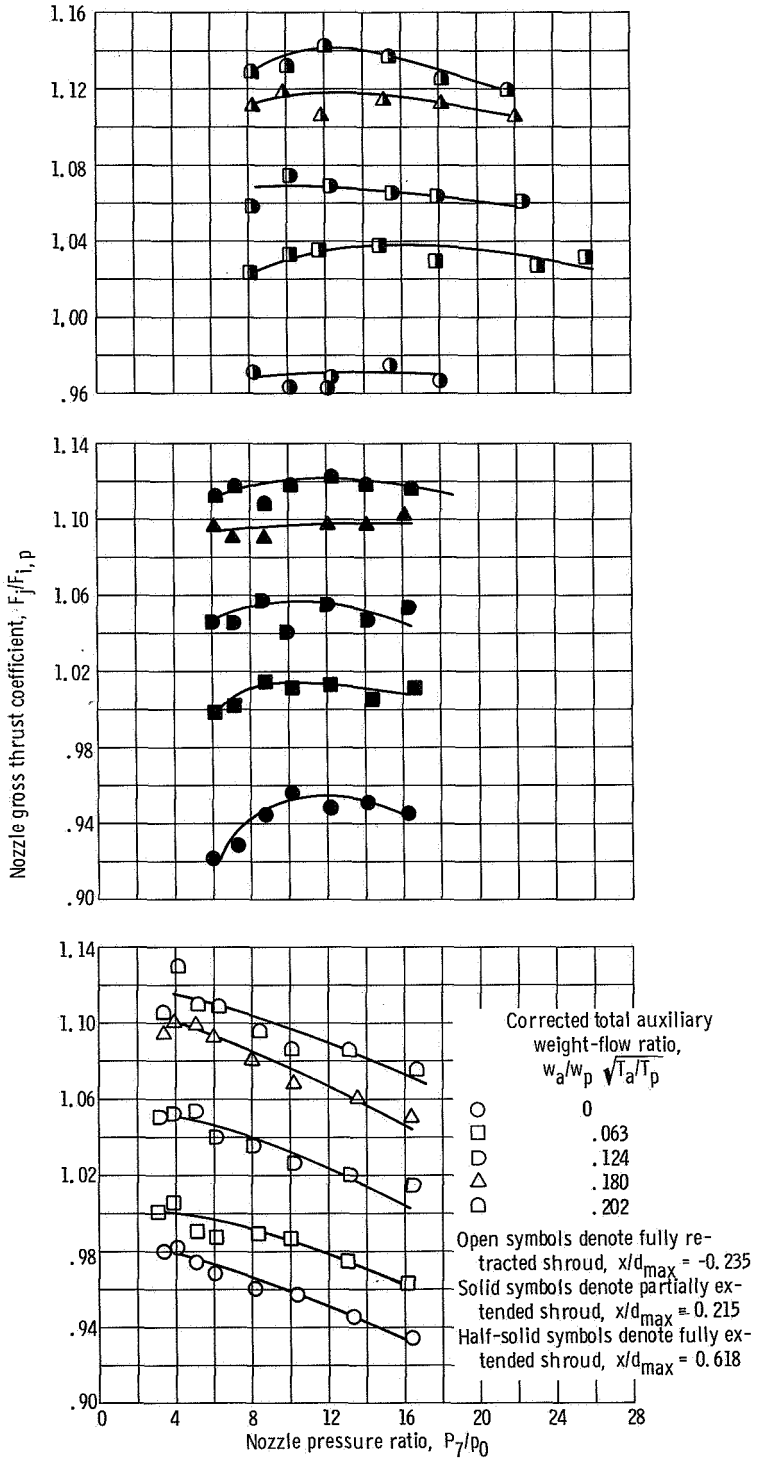

(b) Afterburner on (iris).

Figure 9. - Continued.

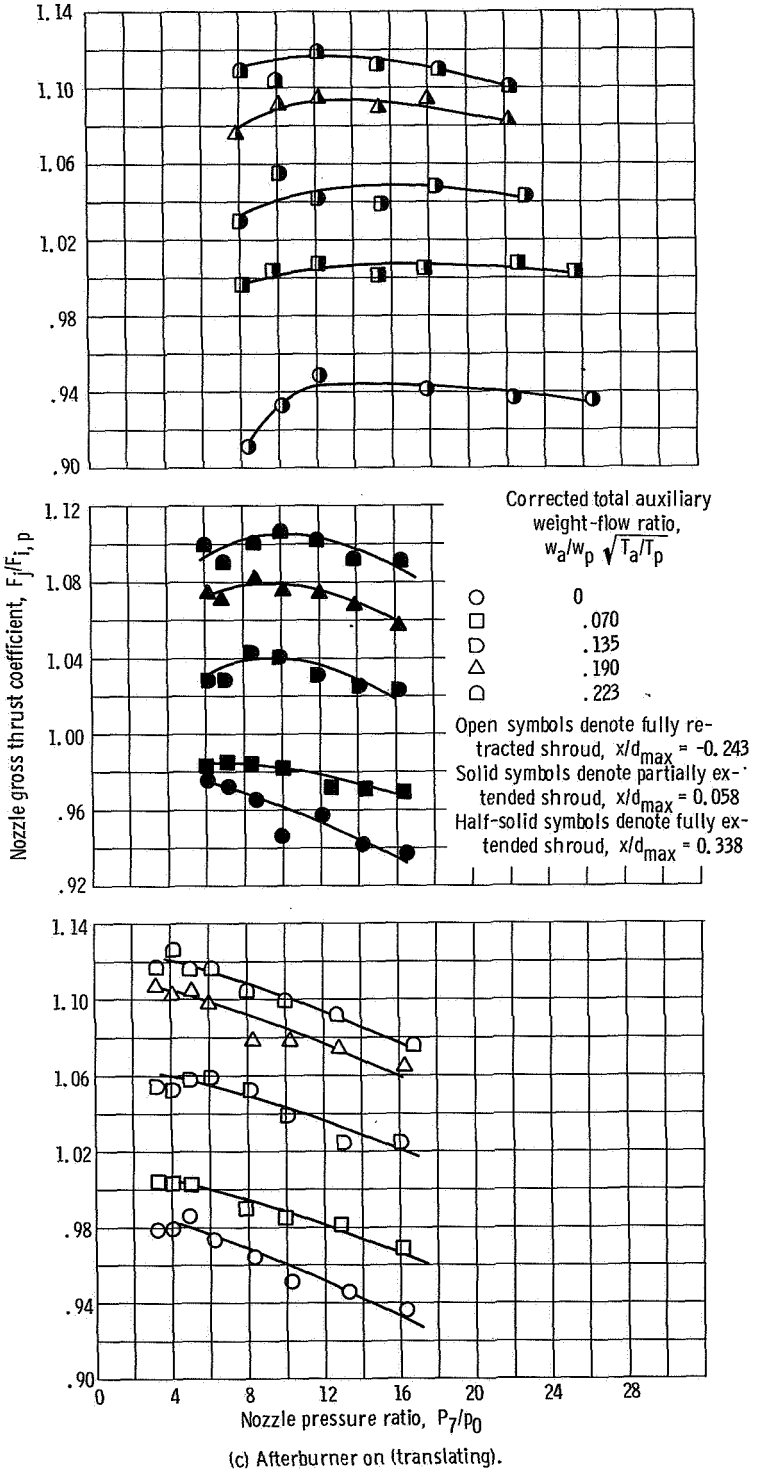

(c) Afterburner on (translating).

Figure 9. - Concluded.

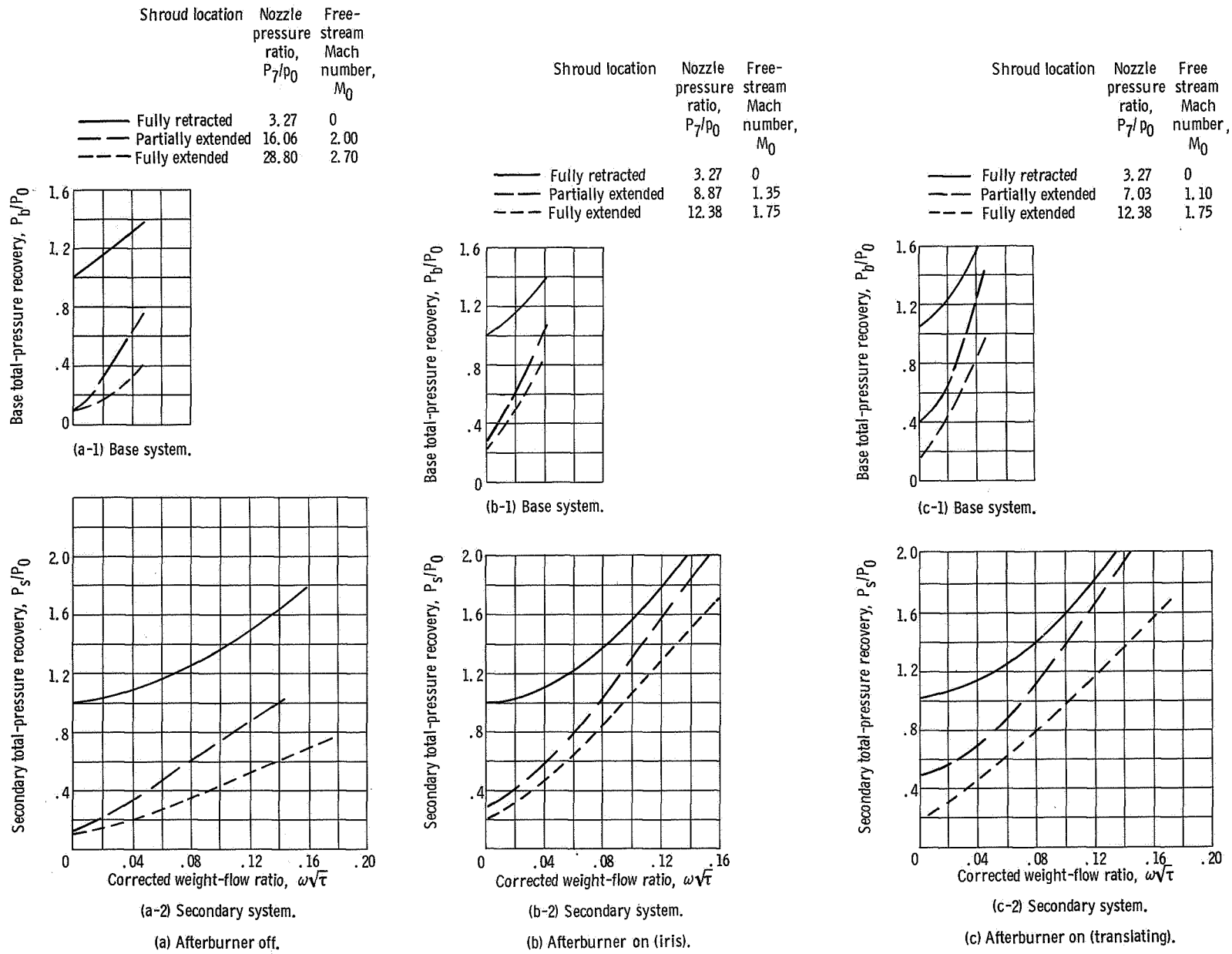

Figure 10. - Total-pressure-recovery requirements for secondary and base weight flows.

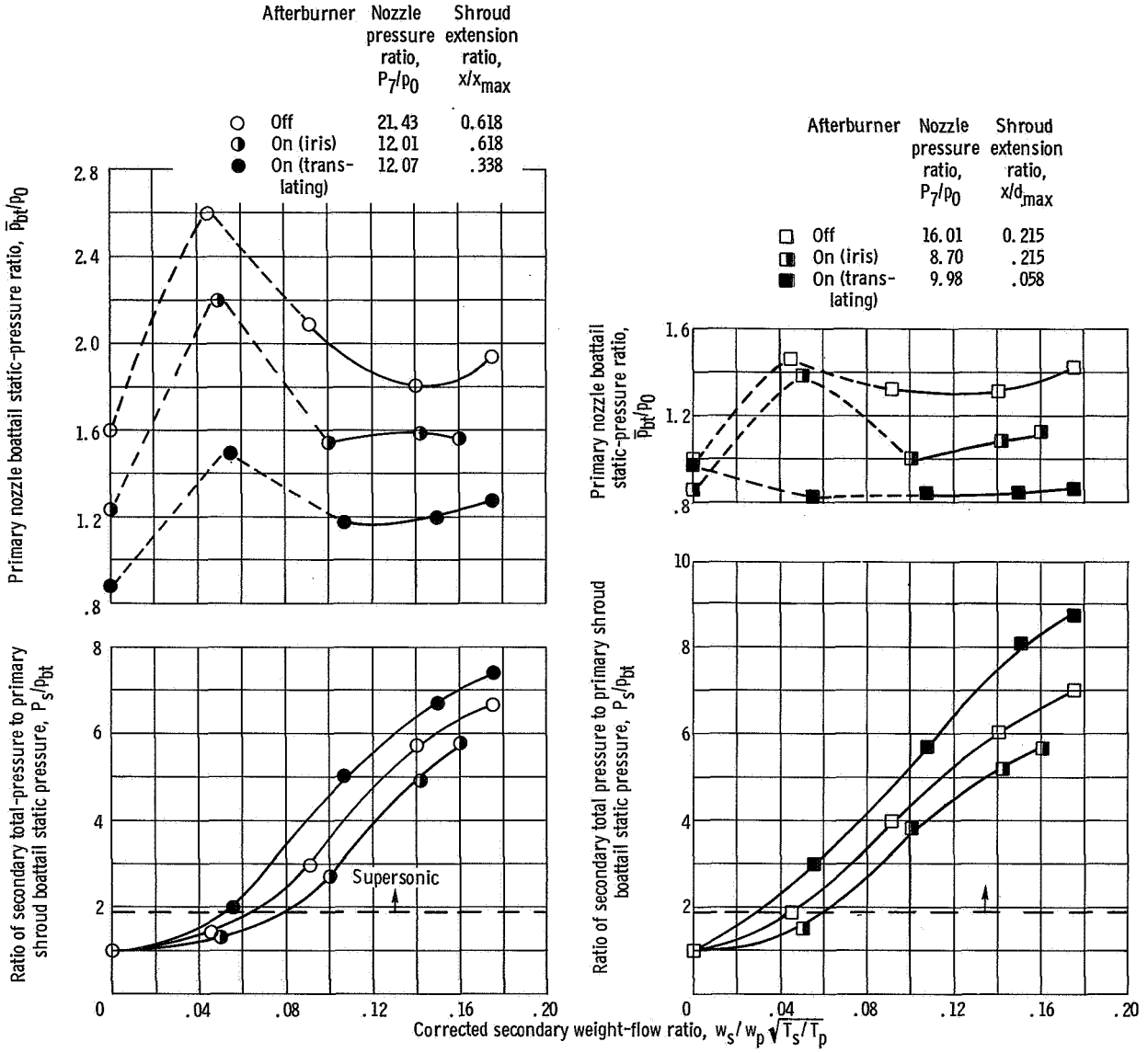

(a) Fully extended shroud.

(b) Partially extended shroud.

Figure 11. - Effect of secondary flow on primary nozzle.

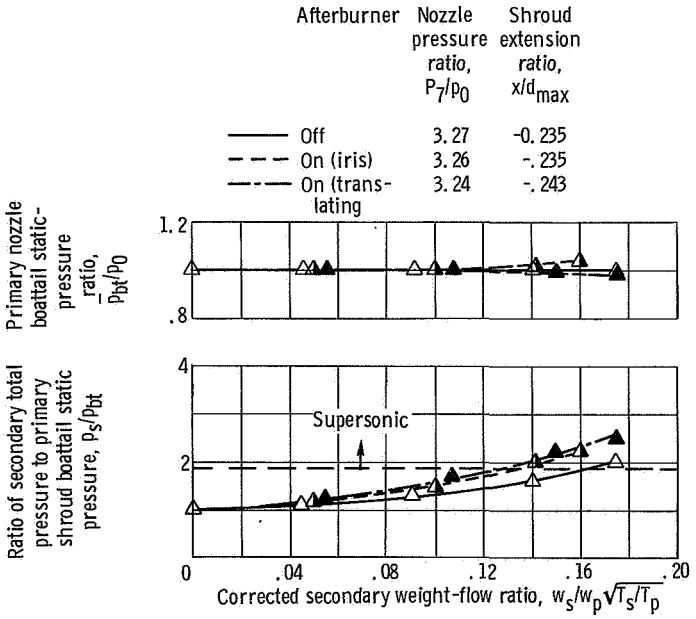

(c) Fully retracted shroud.

Figure 11. - Concluded.

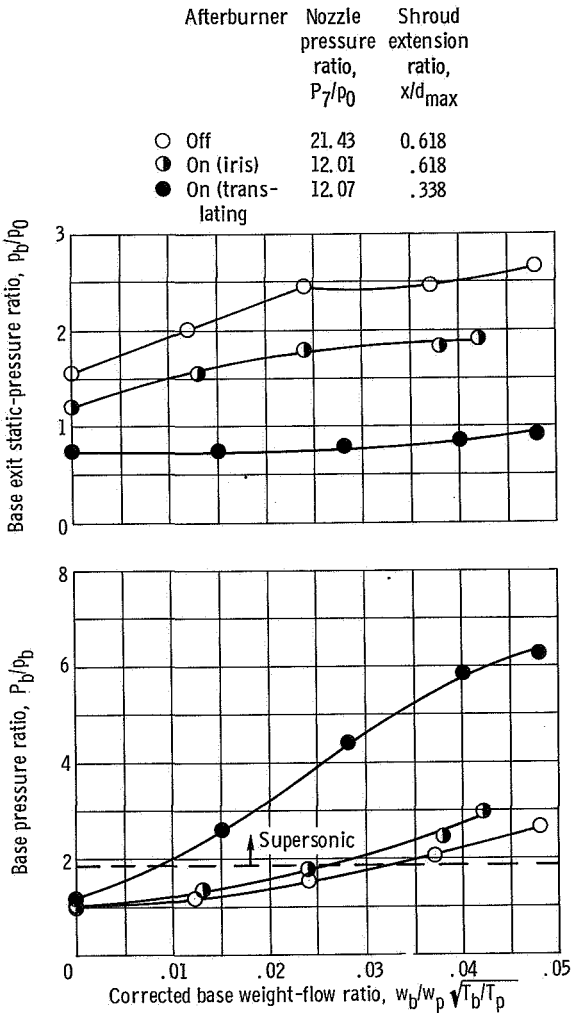

(a) Fully extended shroud.

Figure 12. - Effect of base weight flow on base pressure.

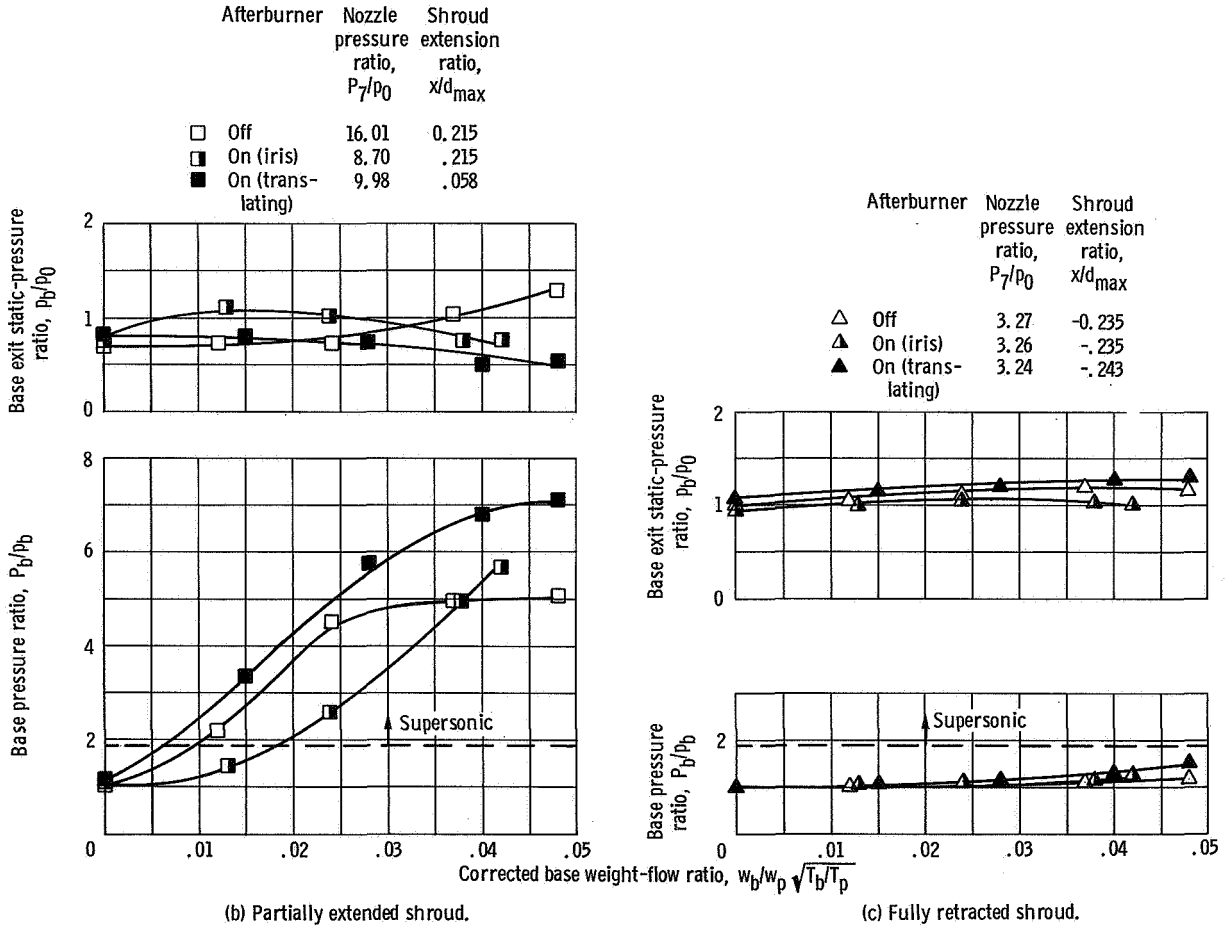

(b) Partially extended shroud.

(c) Fully retracted shroud.

Figure 12. - Concluded.

NATIONAL AERONAUTICS AND SPACE ADMINISTRATION
WASHINGTON, D.C. 20546

OFFICIAL BUSINESS

FIRST CLASS MAIL

POSTAGE AND FEES PAID
NATIONAL AERONAUTICS A
SPACE ADMINISTRATION

POSTMASTER: If Undeliverable (Section 15
Postal Manual) Do Not Retu

"The aeronautical and space activities of the United States shall be conducted so as to contribute . . . to the expansion of human knowledge of phenomena in the atmosphere and space. The Administration shall provide for the widest practicable and appropriate dissemination of information concerning its activities and the results thereof."

— NATIONAL AERONAUTICS AND SPACE ACT OF 1958

NASA SCIENTIFIC AND TECHNICAL PUBLICATIONS

TECHNICAL REPORTS: Scientific and technical information considered important, complete, and a lasting contribution to existing knowledge.

TECHNICAL NOTES: Information less broad in scope but nevertheless of importance as a contribution to existing knowledge.

TECHNICAL MEMORANDUMS: Information receiving limited distribution because of preliminary data, security classification, or other reasons.

CONTRACTOR REPORTS: Scientific and technical information generated under a NASA contract or grant and considered an important contribution to existing knowledge.

TECHNICAL TRANSLATIONS: Information published in a foreign language considered to merit NASA distribution in English.

SPECIAL PUBLICATIONS: Information derived from or of value to NASA activities. Publications include conference proceedings, monographs, data compilations, handbooks, sourcebooks, and special bibliographies.

TECHNOLOGY UTILIZATION PUBLICATIONS: Information on technology used by NASA that may be of particular interest in commercial and other non-aerospace applications. Publications include Tech Briefs, Technology Utilization Reports and Notes, and Technology Surveys.

Details on the availability of these publications may be obtained from:

SCIENTIFIC AND TECHNICAL INFORMATION DIVISION

NATIONAL AERONAUTICS AND SPACE ADMINISTRATION

Washington, D.C. 20546